Available online at www.sciencedirect.com
SCIENCE DIRECT®
Journal of Magnetic Resonance 163 (2003) 310–317
JMR Journal of Magnetic Resonance
www.elsevier.com/locate/jmr

Application of amplitude-modulated radiofrequency fields to the magic-angle spinning NMR of spin-$\frac{7}{2}$ nuclei

P.K. Madhu,[a,1] Ole G. Johannessen,[a] Kevin J. Pike,[b] Ray Dupree,[b] Mark E. Smith,[b] and Malcolm H. Levitt[a,*]

[a] *Department of Chemistry, University of Southampton, Southampton SO17 1BJ, UK*
[b] *Department of Physics, University of Warwick, Coventry CV4 7AL, UK*

Received 28 January 2003; revised 15 April 2003

Abstract

We report pulse sequences for the sensitivity enhancement of magic-angle spinning and multiple-quantum magic-angle spinning spectra of spin-$\frac{7}{2}$ systems. Sensitivity enhancement is obtained with the use of fast amplitude-modulated (FAM) radiofrequency pulses. In one-dimensional magic-angle spinning experiments, signal enhancement of 3 is obtained by a FAM pulse followed by a soft 90° pulse. In two-dimensional multiple-quantum magic-angle spinning experiments, FAM pulses are used for both the excitation of multiple-quantum coherences and for their conversion into observable single-quantum coherences. The observed signal enhancements are 2.2 in 3Q experiments, 3.1 in 5Q experiments, and 4.1 in 7Q experiments, compared to the conventional two-pulse scheme. The pulse schemes are demonstrated on the ^{45}Sc NMR of $Sc_2(SO_4)_3 \cdot 5H_2O$ and the ^{139}La NMR of $LaAlO_3$. We also demonstrate the generation of FAM pulses by double-frequency irradiation.
© 2003 Published by Elsevier Science (USA).

1. Introduction

There are several nuclei with a spin quantum number of $\frac{7}{2}$, and which are of importance in inorganic chemistry, material science, and metalloproteins [1]. Some examples are ^{43}Ca, ^{45}Sc, ^{49}Ti, ^{51}V, ^{59}Co, and ^{139}La. Chemical shift and quadrupolar interaction parameters may be obtained in solid samples by one-dimensional (1D) magic-angle spinning (MAS) [1] and two-dimensional (2D) multiple-quantum magic-angle spinning (MQ-MAS) [2,3] spectroscopy. The 2D MQ-MAS technique provides the nuclear quadrupolar coupling constant χ, asymmetry parameter η_Q, isotropic chemical shift, and quadrupolar shift of individual chemical sites.

MAS and MQ-MAS experiments of spin-$\frac{7}{2}$ systems often suffer from an inherent lack of sensitivity due to the low magnetogyric ratio (e.g., ^{43}Ca, ^{49}Ti) and the large second-order quadrupolar broadening (e.g., ^{49}Ti, ^{139}La). In MQ-MAS, the sensitivity problem is compounded by the inherent difficulty of exciting the higher multiple-quantum orders. In general, the higher the multiple-quantum order, the lower the sensitivity but the better the resolution [4].

Fast amplitude-modulated (FAM) pulses, introduced by Vega and Naor [5], lead to enhancement of both 1D-MAS and MQ-MAS signals [6]. A FAM pulse train when applied before a low-amplitude $\frac{\pi}{2}$ pulse has been shown to give substantial signal enhancement in the 1D-MAS NMR of spin-$\frac{3}{2}$ [7] and spin-$\frac{5}{2}$ quadrupolar nuclear systems [8], compared to the conventional 1D-MAS spectra obtained with a high-amplitude $\frac{\pi}{2}$ pulse. The signal enhancement is brought about by a redistribution in the populations across the satellite transitions [7–9]. This mechanism, called rotor-assisted population transfer (RAPT), generally leads to only a minor distortion of the anisotropic lineshapes [7,8].

FAM pulses also lead to enhanced efficiency in both the excitation of multiple-quantum coherences (MQC) and in the conversion of MQC to one-quantum coher-

* Corresponding author. Fax: +44-23-8059-6753.
E-mail addresses: mhl@soton.ac.uk, Malcolm.Levitt@soton.ac.uk (M.H. Levitt).
[1] Present address: Department of Chemical Sciences, Tata Institute of Fundamental Research, Homi Bhabha Road, Colaba, Mumbai 400 005, India.

1090-7807/$ - see front matter © 2003 Published by Elsevier Science (USA).
doi:10.1016/S1090-7807(03)00159-9

ence (1QC) in spin-$\frac{3}{2}$ and spin-$\frac{5}{2}$ systems [6,10]. However, no FAM signal enhancement schemes have yet been reported for spin-$\frac{7}{2}$ systems. Here, we explore the application of FAM pulses to the signal enhancement of 1D-MAS, 3Q-MAS, 5Q-MAS, and 7Q-MAS spectra in spin-$\frac{7}{2}$ systems. A threefold signal enhancement in 1D-MAS NMR is obtained with a FAM pulse train followed by a soft $\pi/2$ pulse. Experimental results for the ^{139}La NMR of $LaAlO_3$ and the ^{45}Sc NMR of $Sc_2(SO_4)_3 \cdot 5H_2O$ illustrate the RAPT signal enhancement. MQ-MAS signal enhancements by factors between 2 and 4 are obtained for the 3Q-, 5Q-, and 7Q-MAS spectra of ^{139}La nuclei in $LaAlO_3$.

The FAM irradiation is usually generated by amplitude modulation of a single carrier frequency. We also demonstrate a different method for generating the RF modulations, namely by double-frequency irradiation using two independent transmitter channels. This scheme gives comparable signal enhancement to the conventional implementation of FAM.

2. Classification and notation of FAM pulse sequences

Two distinct classes of FAM modulations, called FAM-I and FAM-II, have generally been used in the MAS NMR of half-integer quadrupolar spins [6,11–13]. In order to clarify the discussion, a notation for the sequences is now introduced.

2.1. FAM-I sequences

Fig. 1a shows a schematic of a FAM-I scheme. This involves a train of equally spaced pulses of equal duration and alternating phases of 0 and π (denoted x and $\bar{x}$). In this paper, we denote this type of sequence as $F_n^{\mathrm{I}}(\tau)$ where n corresponds to the number of pulses and τ represents the repetition period. If the pulse duration is τ_{p} and the window interval is τ_{w}, then the period is $\tau = 2\tau_{\mathrm{p}} + 2\tau_{\mathrm{w}}$. The pulse scheme in the figure corresponds to $F_8^{\mathrm{I}}(\tau)$. The scheme $F_n^{\mathrm{I}}(\tau)$ may be treated as a rough approximation to a smoothly modulated cosine wave with a modulation frequency τ^{-1}. FAM-I schemes of this type are used in RAPT experiments and in the conversion of 3QC to observable 1QC in spin-$\frac{3}{2}$ systems [6,12].

We have also generated FAM-I type modulations using double-frequency irradiation, as described below.

For optimum performance on higher half-integer quadrupolar spins, such as spin-$\frac{5}{2}$ and spin-$\frac{7}{2}$, the number of modulation frequencies needs to be increased due to the additional satellite transitions. Better performance for both the 1D-MAS or 2D MQ-MAS experiments is obtained by sequentially perturbing each of the satellite transitions. In a spin-$\frac{n}{2}$ system this may be brought about by $\frac{1}{2}(n-1)$ consecutive FAM trains with different

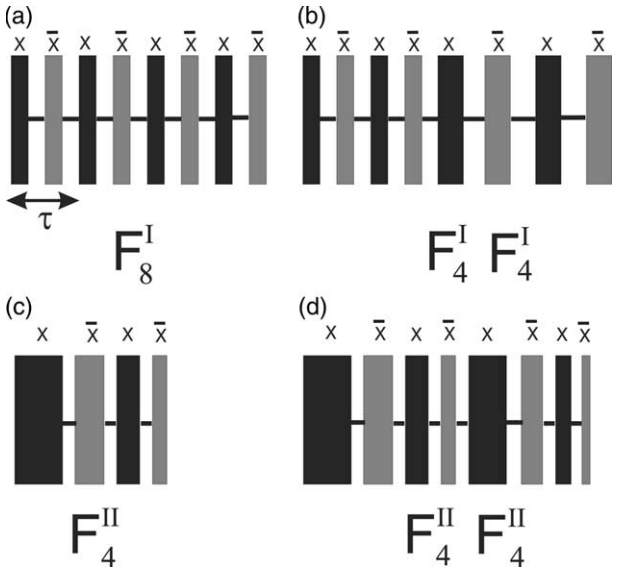

Fig. 1. (a) Schematic of FAM-I with eight pulses with phase 0 and π of equal duration, τ_{p} and separated by an interpulse delay τ_{w}. A sequence of this type is denoted as F_8^{I}. (b) Schematic of two consecutive FAM-I sequences with different modulation frequencies denoted as $F_4^{\mathrm{I}}F_4^{\mathrm{I}}$. (c) Schematic of FAM-II with four pulses of decreasing duration separated by an uniform interpulse delay τ_{w} denoted as F_4^{II}. (d) Schematic of two consecutive FAM-II sequences with different pulse durations denoted as $F_4^{\mathrm{II}}F_4^{\mathrm{II}}$.

periods, i.e., $F_n^{\mathrm{I}}(\tau)F_{n'}^{\mathrm{I}}(\tau')$ as sketched in Fig. 1b. In Fig. 1b, the pulse duration and interpulse delay in the first block are shorter than those in the second block, and hence, this sequence generates a faster modulation of the RF field followed by a slower modulation. Consecutive FAM-I schemes of this type are used in RAPT experiments [8] and in the conversion of 5QC to observable 1QC in the 5Q-MAS of spin-$\frac{5}{2}$ systems [8,14]. In the latter case the consecutive FAM-I pulse trains implement a 5QC $\rightarrow$ 1QC conversion in two steps as 5QC $\rightarrow$ 3QC $\rightarrow$ 1QC.

For brevity, the symbol $F_n^{\mathrm{I}}F_n^{\mathrm{I}}$ is taken to imply two consecutive FAM-I modulation sequences with the same number of pulses n, but different periods.

2.2. FAM-II sequences

In general, FAM-I schemes give good efficiency for conversion of the highest MQC into 1QC. For the conversion of lower-order MQC into 1QC (for example, 3Q-MAS and 5Q-MAS of spin-$\frac{7}{2}$ nuclei), a different type of FAM scheme, namely FAM-II, usually gives better performance.

Fig. 1c shows a schematic of a FAM-II scheme. This consists of a train of pulses of progressively decreasing duration with alternating phases of 0 and π separated by an interpulse delay. Such a FAM-II scheme is denoted here as $F_n^{\mathrm{II}}(\mathbf{T})$ where n corresponds to the number of pulses and $\mathbf{T}$ is a vector containing the pulse and

window durations, $\mathbf{T} = (\tau_p^{(1)}, \tau_w, \tau_p^{(2)}, \ldots, \tau_p^{(n)})$. Normally, the pulses are ordered such that $\tau_p^{(1)} > \tau_p^{(2)} > \tau_p^{(3)} > \cdots > \tau_p^{(n)}$, and all the windows durations τ_w are the same. Odd-numbered pulses are applied with phase 0° and even-numbered pulses are applied with phase π. The FAM-II scheme sketched in Fig. 1c consists of four pulses, and may be denoted as $F_4^{II}(\mathbf{T})$.

In some experiments, two or more consecutive F_n^{II} schemes are needed. This is the case, for example, when the magnitude of the coherence order change is more than 2. Fig. 1d shows an example of a $F_4^{II}F_4^{II}$ scheme involving two consecutive FAM-II pulse trains of different modulation frequencies with four pulses each.

The FAM sequences may be combined with unmodulated RF pulses, denoted here by the symbol P (unmodulated pulses are also called continuous-wave or CW pulses in the literature [6]). We distinguish between high-amplitude "hard" RF pulses (central-transition nutation frequency $\gg$ second-order quadrupolar broadening), which we denote P_H, and "soft" pulses (central-transition nutation frequency $\leqslant$ second-order quadrupolar broadening), denoted here as P_S.

Groups of pulses with an overall 180° phase shift are denoted by an overbar.

3. Experimental

The experiments were performed on ^{139}La nuclei of $LaAlO_3$ and the ^{45}Sc nuclei of $Sc_2(SO_4)_3 \cdot 5H_2O$. The natural abundance of both ^{139}La and ^{45}Sc is ≈100%.

The details of the synthesis of $LaAlO_3$ are as follows. Dry powders of a stoichiometric mixture of Al_2O_3 and La_2O_3 were pressed into a pellet and fired at 1775 °C for 2 h. The pellet was ground, repressed into a new pellet, and fired again under the same conditions. X-ray diffraction showed the sample to be single phase $LaAlO_3$ to better than 98%. There is only one ^{139}La site in this sample with quadrupolar parameters $\chi = 6.0$ MHz, and $\eta_Q \approx 0$ [15].

$Sc_2(SO_4)_3 \cdot 5H_2O$ was purchased from Sigma and used without further treatment. There are three ^{45}Sc sites in this sample with (χ, η_Q) values of (5.2 MHz, 0.1), (4.3 MHz, 0.8) , and (4.5 MHz, 0.5) [4].

The RAPT experiment on $LaAlO_3$ was carried out on a Chemagnetics Infinity 600 spectrometer using a 4 mm probe. The RAPT experiment on $Sc_2(SO_4)_3 \cdot 5H_2O$ was carried out on a Varian Infinity+ 300 spectrometer using a 4 mm probe.

The 3Q-MAS and 5Q-MAS experiments on $LaAlO_3$ were carried out on a Chemagnetics Infinity+ 300 spectrometer using a 4 mm probe. The 7Q-MAS experiment on $LaAlO_3$ was carried out on a Varian Infinity+ 400 spectrometer using a 4 mm probe.

The MAS spinning frequency for all experiments was 10.0 kHz. All hard pulses used a RF field providing a 90° pulse on the central transition of duration 1.67 μs, corresponding to a central-transition nutation frequency of $|(1/2)(I+1/2)\gamma B_{RF}^{peak}|/(2\pi) = 150$ kHz, where B_{RF}^{peak} is the peak RF field strength. All soft pulses used a RF field providing a 90° pulse on the central-transition of duration 5.0 μs, corresponding to a central-transition nutation frequency of 50 kHz. All FAM pulses used a RF field providing a 90° pulse on the central transition of duration 1.67 μs, corresponding to a central-transition nutation frequency of 150 kHz. The MQ-MAS spectra were collected using the whole-echo split-t_1 method [16].

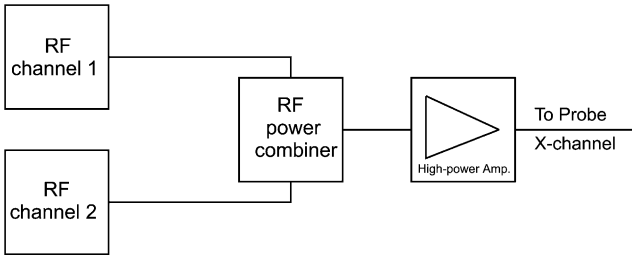

Fig. 2. Block diagram of the double-frequency irradiation hardware.

In one case we used double-frequency irradiation to generate a FAM-I type modulation. In this case, we combined the outputs of two independent spectrometer channels using a commercial power combiner (model ZSC-2-1, Mini Circuits, New York, USA). The combined signal was amplified and fed into the probe. A schematic of the hardware is shown in Fig. 2. The signal outputs taken from the two independent channels 1 and 2 are set to the frequencies $\omega_{ref} \pm \omega_{mod}$ where ω_{ref} is the centre frequency of the irradiation and $\omega_{mod} = 2\pi/\tau$, where τ corresponds to the period of the equivalent FAM-I scheme. In the work done here, we did not synchronise the pulse sequence with the difference frequency of the two channels, so the modulation phase was irreproducible from transient to transient. This did not appear to influence the RAPT enhancement effect. The modulation was terminated by setting the amplitude of one channel to zero and by changing the frequency of the other channel to ω_{ref}.

4. Results and discussions

4.1. One-dimensional MAS spectra

Fig. 3 shows the pulse sequences used for the 1D-MAS NMR of spin-$\frac{7}{2}$ systems. Fig. 3a shows a conventional MAS pulse scheme using a hard $\frac{\pi}{2}$ pulse (P_H) while (b) shows a FAM-MAS scheme of the form $F_n^I(\tau)F_{n'}^I(\tau')P_S$. The second FAM block is modulated slower then the first, i.e. $\tau' > \tau$.

Figs. 3c and d show the ^{139}La MAS spectra of $^{139}LaAlO_3$ obtained using optimised pulse sequences of

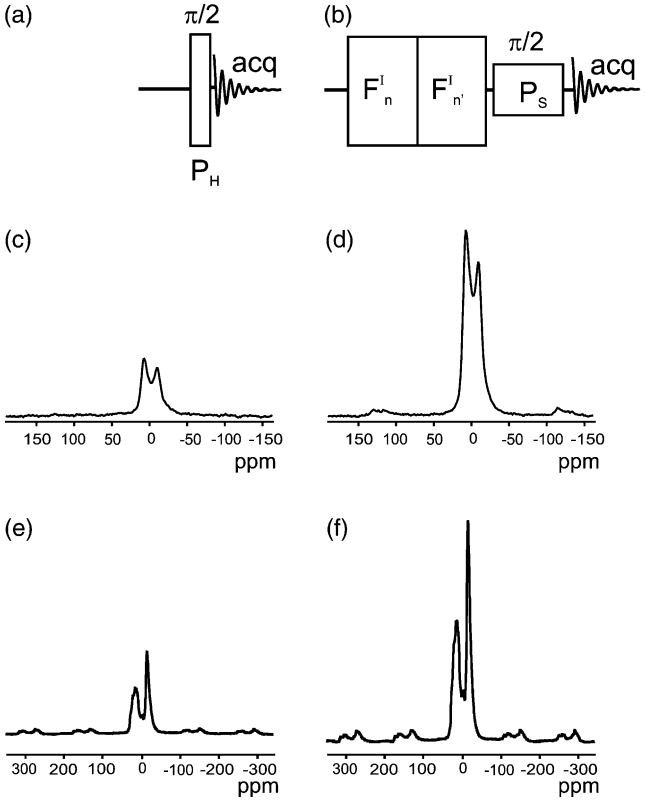

Fig. 3. (a) Conventional pulse sequence for 1D-MAS experiments involving only a single hard $\frac{\pi}{2}$ pulse, denoted P_H. (b) FAM pulses precede a soft $\frac{\pi}{2}$ pulse, denoted P_S, to achieve rotor assisted population transfer, RAPT. (c) and (d) ^{139}La MAS spectrum of $LaAlO_3$ obtained with the pulse sequence in (a) and (b), respectively. The static field was 14.09 T corresponding to a ^{139}La Larmor frequency of −84.746 MHz. (e) and (f) ^{45}Sc MAS spectrum of $Sc_2(SO_4)_3 \cdot 5H_2O$ obtained with the pulse sequence in (a) and (b), respectively. The static field was 7.05 T corresponding to a ^{45}Sc Larmor frequency of −72.863 MHz.

Figs. 3a and b, respectively. The enhancement with FAM in this case is ca. 3.1. All enhancements are defined as the ratio of the enhanced to non-enhanced signal amplitudes. One hundred and sixty transients were collected for both Figs. 3c and d with a recycle delay of 0.5 s.

Figs. 3e and f show the ^{45}Sc MAS spectra of $^{45}Sc_2(SO_4)_3 \cdot 5H_2O$. The signal enhancement in this case is ca. 3.0. Although $Sc_2(SO_4)_3 \cdot 5H_2O$ contains three sites with very different values of χ and η_Q, no significant lineshape distortion is observed in the FAM-enhanced MAS spectrum. Eighty transients were collected for both Figs. 3e and f with a recycle delay of 0.5 s.

The following experimental parameters were employed for the modulations in Figs. 3d and f. The first block, F_n^I, had the following timing parameters: $\tau_p = 0.5\,\mu s$, $\tau_w = 0.5\,\mu s$, and $n = 50$. The second block, $F_{n'}^I$, had the parameters $\tau_{p'} = 1.0\,\mu s$, $\tau_{w'} = 1.0\,\mu s$, and $n' = 50$. The FAM periods were $\tau = 2\,\mu s$ and $\tau' = 4\,\mu s$.

The optimisation protocol for the spectra in Fig. 3 was as follows. The P_H pulse was calibrated by adjusting

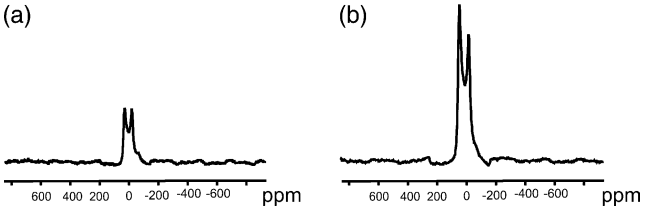

Fig. 4. (a) ^{139}La MAS spectrum of $LaAlO_3$ obtained using the sequence in Fig. 3a. (b) RAPT enhanced ^{139}La MAS spectrum of $LaAlO_3$ obtained using the sequence in Fig. 3b where the FAM pulses were generated by double-frequency irradiation. The static field was 7.05 T corresponding to a ^{139}La Larmor frequency of −42.37 MHz.

the pulse duration and RF field strength so as to give maximum signal in the conventional single-pulse experiment of Fig. 3a. The central-transition nutation frequency for the soft pulse, P_S, was set to about 1/3 of this value. A FAM block of the form $F_{n'}^I$ was inserted before the pulse P_S with the pulse duration and interpulse delay both set to 1 μs. These were varied together with n' in order to optimise the signal. A second FAM block of the form F_n^I was then inserted before the optimised $F_{n'}^I$. The pulse duration and interpulse delay in this block were then decreased, keeping $n = n'$, until a maximum signal enhancement was obtained.

The double-frequency irradiation scheme sketched in Fig. 2 is demonstrated in Fig. 4. Fig. 4a shows the ^{139}La spectrum of $LaAlO_3$ obtained with the pulse sequence in Fig. 3a, and Fig. 4b shows the ^{139}La spectrum of $LaAlO_3$ obtained with the pulse sequence in Fig. 3b where double-frequency irradiation was used to generate the FAM-I sequence. The modulation frequencies corresponded to 600 and 350 kHz both applied for 100 μs. The amplitude of both modulation components corresponded to a central-transition nutation frequency of 150.0 kHz. The enhancement factor is ca. 3.0 which is comparable with that obtained with FAM-I sequences generated in the usual way. The following experimental parameters were used: MAS frequency of 10.0 kHz, central-transition nutation frequency of P_H at 150.0 kHz, central-transition nutation frequency of P_S at 50.0 kHz, 160 transients were collected in both Figs. 4a and b with a relaxation delay of 0.5 s.

At this point, we have not identified any advantages of the double-frequency irradiation scheme over the amplitude modulation method.

The enhancement of 1D MAS signals of spin-$\frac{5}{2}$ systems by a factor of ca. 2.5 [8] and of spin-$\frac{7}{2}$ systems by a factor of ca. 3.0 indicates that the routine use of FAM schemes is beneficial for a large range of half-integer spin systems.

4.2. Three-quantum magic-angle spinning

The split-t_1 whole-echo scheme [16] with FAM pulses for 3Q-MAS experiments in spin-$\frac{7}{2}$ systems is shown in

Fig. 5. This 3Q-MAS pulse sequence uses an unmodulated pulse, P_H, for the excitation of 3QC and a FAM-II sequence for the conversion of 3QC into observable 1QC.

Fig. 6a shows the 2D ^{139}La 3Q-MAS spectrum of $LaAlO_3$ obtained with the conventional two-pulse P_H–P_H scheme of Frydman and Harwood [2]. The pulse durations were 5.1 μs for the first hard pulse and 1.8 μs for the second hard pulse, and were estimated by maximising the 3Q-filtered signal amplitude for a short t_1 value of 5.0 μs. The isotropic and anisotropic projections are shown in Figs. 6b and c.

Fig. 6d shows the 2D ^{139}La 3Q-MAS spectrum of $LaAlO_3$ obtained with the P_H–F_2^{II} scheme of Fig. 5. The isotropic and anisotropic projections are shown in Figs. 6e and f. The spectrum is more intense by a factor of 2.0 compared to that obtained with the conventional two-pulse method. The FAM pulses give rise to relatively undistorted anisotropic lineshapes in addition to the signal enhancement.

Both 2D spectra in Fig. 6 were acquired with a 96-step nested phase cycle using 192 transients per t_1 increment. Two hundred and fifty six t_1 acquisitions were collected with a t_1 increment of 5 μs, and a t_2 increment of 50 μs. The recycle delay was 0.5 s.

The optimisation protocol for the P_H–F_2^{II} sequence was as follows. The optimal pulse duration of 5.1 μs in the two-pulse P_H–P_H experiment was used for the first pulse. The F_2^{II} sequence was optimised by setting the first hard pulse to $\tau_p^{(1)} = 1.8\,\mu s$ and then adjusting the second pulse duration $\tau_p^{(2)}$ for the maximum 3Q echo intensity for an evolution interval $t_1 = 5.0\,\mu s$, keeping the window interval $\tau_w = 0.2\,\mu s$. The optimum value was found to be $\tau_p^{(2)} = 1.4\,\mu s$. No further enhancement of the 3Q echo signal was obtained by adding further pulses to the F_2^{II} block. The optimum conversion block was therefore $F_2^{II}(\mathbf{T})$, with $\mathbf{T} = \{1.8, 0.2, 1.4\}\,\mu s$.

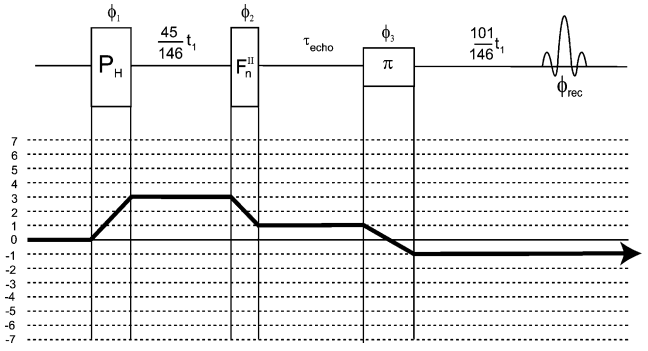

Fig. 5. (a) P_H–F_n^{II} pulse sequence used for the sensitivity-enhanced 3Q-MAS of spins-$\frac{7}{2}$. The coherence pathway leading to a high-resolution 3Q-MAS spectrum is shown.

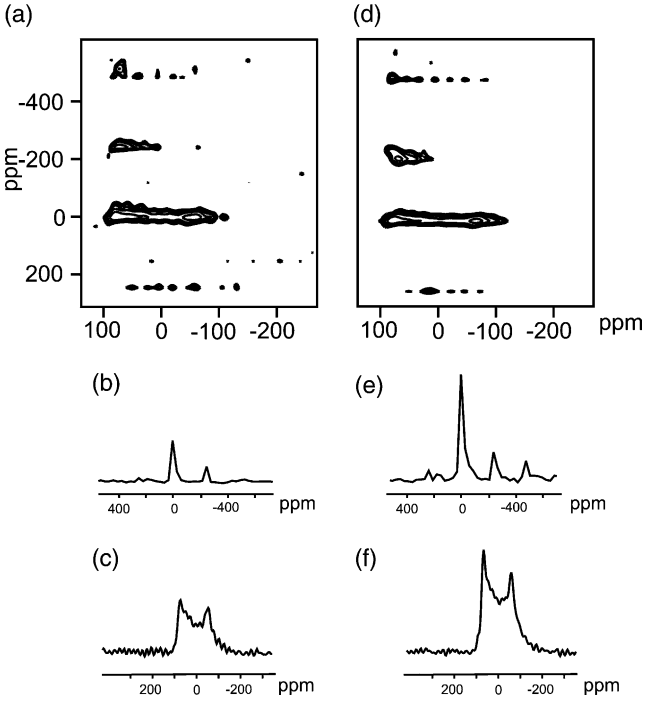

Fig. 6. (a) ^{139}La 2D 3Q-MAS spectrum of $LaAlO_3$ acquired with the conventional two-pulse scheme. (b) and (c) Isotropic and anisotropic projections of the 2D spectrum in (a). (d) ^{139}La 2D 3Q-MAS spectrum of $LaAlO_3$ acquired with $P_H F_2^{II}$ scheme. (e) and (f) Isotropic and anisotropic projections of the 2D spectrum in (d). The spectra were obtained at a static field of 7.05 T corresponding to a ^{139}La Larmor frequency of −42.37 MHz.

4.3. Five-quantum magic-angle spinning

The split-t_1 whole-echo scheme [16] with FAM pulses for 5Q-MAS experiments in spin-$\frac{7}{2}$ systems is shown in Fig. 7. This 5Q-MAS pulse sequence uses a hard unmodulated pulse, P_H, for the excitation of 3QC followed by a $\overline{F_n^I}$ scheme for converting 3QC into 5QC. The conversion of 5QC into observable 1QC is brought about by two consecutive FAM-II sequences. The overall scheme, denoted as $P_H\overline{F_n^I}$–$F_{n'}^{II}F_{n''}^{II}$, is similar to that used in the 5Q-MAS of spin-$\frac{5}{2}$ [17,18].

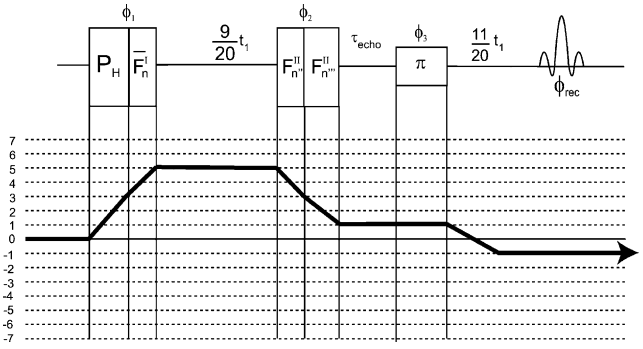

Fig. 7. (a) $P_H\overline{F_n^I}$–$F_{n'}^{II}F_{n''}^{II}$ pulse sequence used for the sensitivity-enhanced 5Q-MAS of spins-$\frac{7}{2}$. The coherence pathway leading to a high-resolution 5Q-MAS spectrum is shown.

Fig. 8a shows the ^{139}La 2D 5Q-MAS spectrum of $LaAlO_3$ obtained with the conventional two-pulse method. The pulse durations were 4.8 μs for the first pulse and 2.2 μs for the second pulse, and were optimised by monitoring the 5Q echo intensity for a short 5Q evolution time of 5.0 μs. The isotropic and anisotropic projections are shown in Figs. 8b and c.

Fig. 8d shows the ^{139}La 2D 5Q-MAS spectrum of $LaAlO_3$ obtained with an optimised $P_H\overline{F_2^I}$–$F_2^{II}F_2^{II}$ scheme. The isotropic and anisotropic projections are shown in Figs. 8e and f. The spectrum is more intense by a factor of 3.0 compared with that obtained with the conventional two-pulse method. The lineshapes of Figs. 8c and f are quite similar, indicating that the enhancement is not accompanied by appreciable lineshape distortions.

Both 2D spectra in Fig. 8 were acquired with a 160-step nested phase cycle using 480 transients per t_1 increment. One hundred and twenty eight t_1 acquisitions were collected with a t_1 increment of 5 μs, and a t_2 increment of 50 μs. The recycle delay was 0.5 s.

The optimisation protocol for the $P_H\overline{F_n^I} - F_{n'}^{II}F_{n''}^{II}$ sequence was as follows. The $\overline{F_n^I}$ sequence was omitted at first and the duration of the P_H pulse was set to 4.8 μs, as in the optimised first pulse of the conventional two-pulse P_H–P_H sequence. The $5Q \rightarrow 1Q$ conversion block was first set to a single $F_{n'}^{II}$ sequence, with the first pulse in that block set to $\tau_p^{(1)} = 2.2\,\mu s$, as in the second pulse of the optimised two-pulse P_H–P_H sequence. The second pulse in the $F_{n'}^{II}$ was then optimised, using an interpulse delay of $\tau_w = 0.2\,\mu s$. This lead to the value $\tau_p^{(2)} = 1.4\,\mu s$ for the second pulse. Addition of further pulses did not increase the signal amplitudes further. A second FAM-II sequence was added using a similar optimisation protocol. The FAM-I block was then inserted and optimised leading to values $\tau_p = \tau_w = 0.6\,\mu s$. The final parameters for the optimal pulse sequence were $P_H\overline{F_2^I}(2.4\,\mu s)$–$F_2^{II}(\mathbf{T})F_2^{II}(\mathbf{T}')$ with $\mathbf{T} = \{2.2, 0.2, 1.4\}\,\mu s$, and $\mathbf{T}' = \{1.8, 0.2, 1.0\}\,\mu s$.

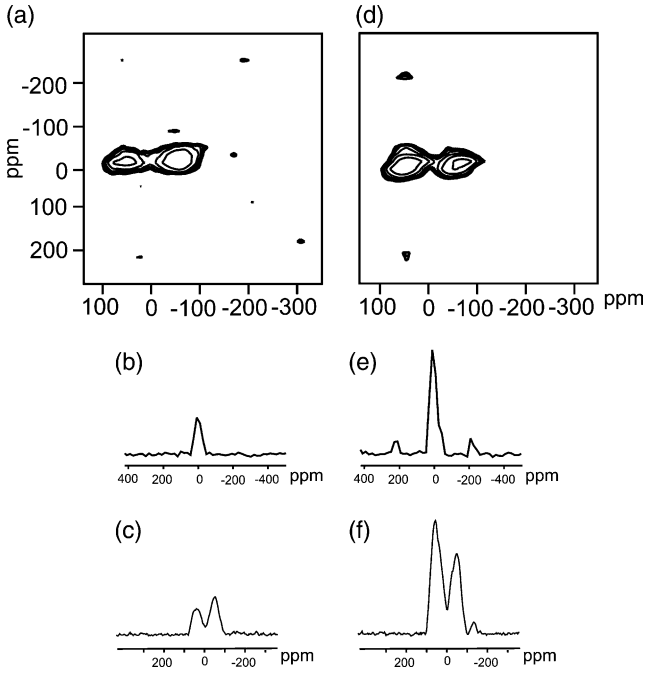

Fig. 8. (a) ^{139}La 2D 5Q-MAS contour spectrum of $LaAlO_3$ acquired with the conventional two-pulse scheme. (b) and (c) Isotropic and anisotropic projections of the 2D spectrum in (a). (d) ^{139}La 2D 5Q-MAS spectrum of $LaAlO_3$ acquired with the $P_H\overline{F_n^I}$–$F_{n'}^{II}F_{n''}^{II}$ scheme. (e) and (f) Isotropic and anisotropic projections of the 2D spectrum in (d). The spectra were obtained at a static field of 7.05 T corresponding to a ^{139}La Larmor frequency of −42.37 MHz.

4.4. Seven-quantum magic-angle spinning

The split-t_1 whole-echo scheme [16] with FAM pulses used for 7Q-MAS experiments in spin-$\frac{7}{2}$ systems is shown in Fig. 9. This 7Q-MAS pulse sequence uses a hard unmodulated pulse for the excitation of 3QC followed by two consecutive FAM-I sequences $\overline{F_n^I}\overline{F_{n'}^I}$, that convert 3QC into 7QC. The conversion of 7QC into observable 1QC is brought about by two consecutive FAM-I sequences. The overall scheme, denoted as $P_H\overline{F_n^I}\overline{F_{n'}^I}$–$F_{n''}^I F_{n'''}^I$, is a minor modification of that used by Goldbourt and Vega [17] for the 5QMAS of spin-$\frac{5}{2}$.

Fig. 10a shows the ^{139}La 2D 7Q-MAS spectrum of $LaAlO_3$ obtained with the conventional two-pulse P_H–P_H method. The pulse durations were 4.0 and 2.1 μs for the first and second pulses, respectively. The optimisation was done by monitoring the 7Q echo intensity for a short 7Q evolution time of 5 μs. The isotropic and anisotropic projections are shown in Figs. 10b and c.

Fig. 10d shows the ^{139}La 2D 7Q-MAS spectrum of $LaAlO_3$ obtained with the $P_H\overline{F_4^I F_4^I}$–$F_8^I F_8^I$ scheme. The isotropic and anisotropic projections are shown in Figs. 10e and f. The spectrum is more intense by a factor of 4.0 compared with that obtained with the conventional two-pulse method. The lineshapes of Figs. 10c and f are quite similar, indicating that the enhancement is not accompanied by appreciable lineshape distortions.

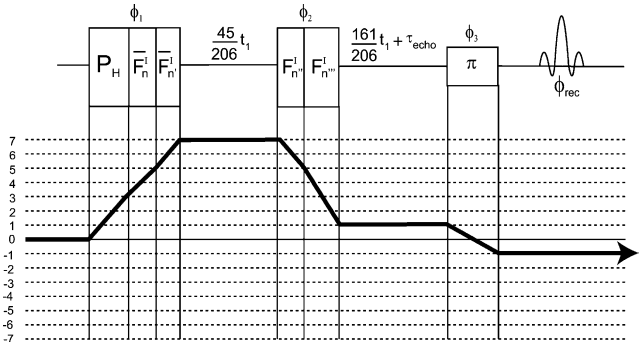

Fig. 9. (a) $P_H\overline{F_n^I}\overline{F_{n'}^I}$–$F_{n''}^I F_{n'''}^I$ pulse sequence used for the sensitivity-enhanced 7Q-MAS spectrum of spins-$\frac{7}{2}$. The coherence pathway leading to a high-resolution 7Q-MAS spectrum is shown.

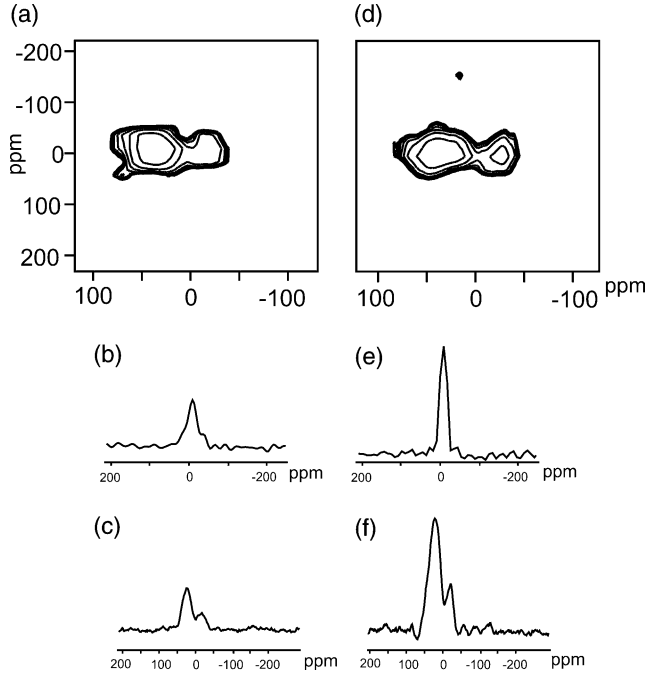

Fig. 10. (a) ^{139}La 2D 7Q-MAS spectrum of $LaAlO_3$ acquired with the conventional two-pulse scheme. (b) and (c) Isotropic and anisotropic projections of the 2D spectrum in (a). (d) ^{139}La 2D 7Q-MAS spectrum of $LaAlO_3$ acquired with the $P_H\overline{F_n^I F_{n'}^I}$–$F_{n''}^I F_{n'''}^I$ scheme. (e) and (f) Isotropic and anisotropic projections of the 2D spectrum in (d). The spectra were obtained at a static field of 9.39 T corresponding to a ^{139}La Larmor frequency of −56.496 MHz.

Both 2D spectra in Fig. 10 were acquired with a 224-step nested phase cycle using 2240 transients per t_1 increment. Thirty-two t_1 acquisitions were collected with a t_1 increment of 5 μs, and a t_2 increment of 50 μs. The recycle delay was 0.5 s.

The $P_H\overline{F_n^I F_{n'}^I}$–$F_{n''}^I F_{n'''}^I$ sequence was optimised by starting first with the simplified sequence P_H–$F_{n''}^I$, and then progressively adding elements as follows: P_H–$F_{n''}^I F_{n'''}^I$, $P_H\overline{F_n^I}$–$F_{n''}^I F_{n'''}^I$, and $P_H\overline{F_n^I F_{n'}^I}$–$F_{n''}^I F_{n'''}^I$. The end point of each optimisation was used as the starting point of the optimisation for the next sequence. The optimised pulse sequence parameters used for the spectrum in Figs. 10d–f were as follows: initial hard pulse duration $\tau_p = 4.0\,\mu s$; first FAM-I sequence, $\overline{F_4^I}$ with $\tau_p = \tau_w = 1.5\,\mu s$; second FAM-I sequence, $\overline{F_4^I}$ with $\tau_p = \tau_w = 1.0\,\mu s$; third FAM-I sequence, F_8^I with $\tau_p = \tau_w = 0.6\,\mu s$; fourth FAM-I sequence, F_8^I with $\tau_p = \tau_w = 1.2\,\mu s$. The optimised pulse sequence can be denoted $P_H\overline{F_4^I}(4.8\,\mu s)\overline{F_4^I}(2.4\,\mu s)$–$F_8^I(6.0\,\mu s)F_8^I(4.0\,\mu s)$.

5. Conclusions

Experimental schemes involving fast amplitude-modulated pulses for the enhancement of 1D-MAS and MQ-MAS spectra of spin-$\frac{7}{2}$ in solids have been presented. The signal enhancements are of the order of 3 for 1D-MAS experiments, and 2.2, 3.1, and 4.1 for 2D 3Q-, 5Q-, and 7Q-MAS experiments, respectively. In MQ-MAS experiments, FAM schemes have been used for both the excitation of 3Q-, 5Q- and 7Q-coherences, and also for the conversion of MQC into observable 1QC. This work together with [7,8] shows that FAM schemes can give substantial signal enhancements in the MAS spectra of all half-integer quadrupolar spins in solids.

It is difficult to compare accurately the absolute signal strengths of MAS spectra with different MQ orders, since the conditions were not identical for all experiments, but a rough estimate indicates that the approximate ratio of FAM-enhanced 3Q:5Q:7Q signal amplitudes was 1:0.4:0.15.

Acknowledgments

We thank Andrew Howes (Warwick) for technical assistance and Allan Baldwin (Warwick) for help with sample manufacture. Helpful discussions with Amir Goldbourt, Shimon Vega, and Thomas Bräuniger are gratefully acknowledged. This research was supported by the EPSRC (UK). K.J.P., R.D. and M.E.S. acknowledge partial support of this work through Grant GR/N29549.

References

[1] K.J.D. MacKenzie, M.E. Smith, Multinuclear Solid-State NMR of Inorganic Materials, Pergamon Press, Oxford, 2002.
[2] L. Frydman, J.S. Harwood, Isotropic spectra of half-integer quadrupolar spins from bidimensional magic-angle spinning NMR, J. Am. Chem. Soc. 117 (1995) 5367–5368.
[3] A. Medek, J.S. Harwood, L. Frydman, Multiple-quantum magic-angle spinning NMR: a new method for the study of quadrupolar nuclei in solids, J. Am. Chem. Soc. 117 (1995) 12779–12787.
[4] K.J. Pike, R.P. Malde, S.E. Ashbrook, J. McManus, S. Wimperis, Multiple-quantum MAS NMR of quadrupolar nuclei. Do five-, seven-, and nine-quantum experiments yield higher resolution than the three-quantum experiment?, Solid State Nucl. Magn. Reson. 16 (2000) 203–215.
[5] S. Vega, Y. Naor, Triple quantum NMR on spin systems with $I = \frac{3}{2}$ in solids, J. Chem. Phys. 75 (1981) 75–86.
[6] A. Goldbourt, P.K. Madhu, Multiple-quantum magic-angle spinning: high-resolution solid state NMR spectroscopy of half-integer quadrupolar nuclei, Chem. Mon. 133 (2002) 1497–1534.
[7] Z. Yao, H.-T. Kwak, D. Sakellariou, L. Emsley, P.J. Grandinetti, Sensitivity enhancement of the central transition NMR signal of quadrupolar nuclei under magic-angle spinning, Chem. Phys. Lett. 327 (2000) 85–90.
[8] P.K. Madhu, K.J. Pike, R. Dupree, M.H. Levitt, M.E. Smith, Modulation aided signal enhancement in the magic angle spinning NMR of spin-$\frac{5}{2}$ nuclei, Chem. Phys. Lett. 367 (2003) 150–156.
[9] D. Iuga, A.P.M. Kentgens, Influencing the satellite transitions of half-integer quadrupolar nuclei for the enhancement of magic angle spinning spectra, J. Magn. Reson. 158 (2002) 65–72.

[10] L. Frydman, Fundamentals of multiple quantum magic angle spinning NMR on half-integer quadrupolar nuclei, in: D.M. Grant, R.K. Harris (Eds.), Encyclopedia of NMR, Suppl. 9, Wiley, Chichester, 2002.
[11] P.K. Madhu, A. Goldbourt, L. Frydman, S. Vega, Sensitivity enhancement of the MQMAS NMR experiment by fast amplitude modulation of the pulses, Chem. Phys. Lett. 307 (1999) 41–47.
[12] P.K. Madhu, A. Goldbourt, L. Frydman, S. Vega, Fast radio-frequency amplitude modulation in multiple-quantum magic-angle-spinning nuclear magnetic resonance: theory and experiments, J. Chem. Phys. 112 (2000) 2377–2391.
[13] A. Goldbourt, P.K. Madhu, S. Vega, Enhanced conversion of triple to single-quantum coherence in the triple-quantum MAS NMR spectroscopy of spin-5/2 nuclei, Chem. Phys. Lett. 320 (2000) 448–456.
[14] T. Vosegaard, D. Massiot, P.J. Grandinetti, Sensitivity enhancement in MQ-MAS NMR of spin-5/2 nuclei using modulated rf mixing pulses, Chem. Phys. Lett. 326 (2000) 454–460.
[15] R. Dupree, M.H. Lewis, M.E. Smith, A high-resolution NMR study of the La–Si–Al–O–N system, J. Am. Chem. Soc. 111 (1989) 5125–5132.
[16] S.P. Brown, S. Wimperis, Two-dimensional MAS multiple-quantum NMR of quadrupolar nuclei. Removal of inhomogeneous second-order broadening, J. Magn. Reson. A119 (1997) 280–284.
[17] A. Goldbourt, S. Vega, Signal enhancement in 5QMAS spectra of spin-5/2 quadrupolar nuclei, J. Magn. Reson. 154 (2002) 280–286.
[18] T. Bräuniger, K.J. Pike, R.K. Harris, P.K. Madhu, Efficient 5QMAS NMR of spin-5/2 nuclei: use of amplitude modulated radiofrequency pulses and cogwheel phase cycling, J. Magn. Reson., in press.